FOREX Publication
Open Access | Rapid and quality publishing
International Journal of Electrical and Electronics Research (IJEER)
Review Article | Volume 13, Issue 1 | Pages 156-163 | e-ISSN: 2347-470X

Simulation and Modeling of Position Control for an X-Configuration Quadcopter Using PID Controller

Sereyvatha Sarin[1*], Chivon Choeung[2], Sophyn Srey[3], and Sarot Srang[4]

[1]*Graduate School, National Polytechnic Institute of Cambodia; sereivatha@yahoo.com*
[2]*Faculty of Electricity, National Polytechnic Institute of Cambodia; choeungchivon@npic.edu.kh*
[3]*Department of Industrial and Mechanical Engineering, Institute of Technology of Cambodia; sophynkh@gmail.com*
[4]*Department of Industrial and Mechanical Engineering, Institute of Technology of Cambodia; srangsarot@itc.edu.kh*

***Correspondence:** *sereivatha@yahoo.com*

ABSTRACT- Quadcopters are gaining popularity in UAV platforms within the control community because of their intricate dynamics and significant potential in outside applications, owing to their advantages over conventional aerial vehicles. This work introduces the mathematical modeling of a basic quadcopter using an X-configuration and simulates its target position using MATLAB. A Proportional-Integral-Derivative (PID) controller is designed for controlling the position and stabilizing the attitude of the quadcopter. The quadcopter's underactuated nature allows this PID controller to maneuver the vehicle in three dimensions and adjust the yaw angle to the required values while stabilizing the pitch and roll angles. The controller's performance and robustness are assessed through simulations using MATLAB and Simulink. The results illustrate the efficacy and quality of PID control in the positioning regulation of a quadcopter.

Keywords: UAV, quadcopter; control, PID, X-configuration, MATLAB, Simulink.

ARTICLE INFORMATION

Author(s): Sereyvatha Sarin, Chivon Choeung, Sophyn Srey, and Sarot Srang;
Received: 18/10/2024; **Accepted**: 27/01/2025; **Published**: 30/03/2025;
e-ISSN: 2347-470X;
Paper Id: IJEER 1810-14;
Citation: 10.37391/IJEER.130120
Webpage-link:
https://ijeer.forexjournal.co.in/archive/volume-13/ijeer-130120.html

crossref member
CROSSREF.ORG
THE CITATION LINKING BACKBONE

Publisher's Note: FOREX Publication stays neutral with regard to Jurisdictional claims in Published maps and institutional affiliations.

1. INTRODUCTION

With rapid growth over the years, quadcopters or drones find their extended use in different industries by offering innovative solutions for various real-world applications. They are used for precision farming by monitoring crop health, controlling irrigation, and even spreading fertilizers or pesticides highly efficiently with very minimal negative impact on the environment [1]. In logistics, it has transformed the delivery mechanism wherein companies like Amazon test drones for parcel delivery, shortening delivery time for consumers significantly. In construction, quadcopters are put into use for surveying lands, inspecting structures, and even monitoring construction in progress-a much safer way out and efficient compared to the conventional methods [2]. Moreover, search and rescue operations [3] have felt the great advantage of quadcopters in situations requiring fast access to impassable or hazardous areas due to their real-time, high-value aerial footage that has been helpful in guiding rescuers. These examples, therefore, outline a wide potential for quadcopters to make enhancements in productivity, safety, and precision across different industries. The rapid invasion into these industries is a strong motivation to further research in enhancing the performance, efficiency, and capabilities of drones. Due to the unmanned aerial vehicles (UAVs) has led to significant advancements in quadcopter technology, particularly in the development of control systems that ensure stability, precision, and adaptability [4]. Among these UAVs, the X-configuration quadcopter stands out due to its superior maneuverability and stability, making it a popular choice for various applications, from surveillance to delivery services [5]. However, achieving precise position control of an X-configuration quadcopter poses substantial challenges due to its highly nonlinear dynamics and susceptibility to external disturbances [6].

Traditional Proportional-Integral-Derivative (PID) controllers are often utilized for quadcopter regulation owing to its simplicity and efficacy across several applications [7]. To address these limitations, there is a growing interest in integrating intelligent control strategies that can adapt to varying conditions and enhance performance. A study on quadcopter-based object detection and localization has been proposed in [8], where an X-configuration quadcopter was integrated with an IP camera for object detection based on the color of an object. While [9] proposing a self-tuning PID control for wind energy conversion system using Lyapunov method. This self-tuning PID control system comprises two controllers: a self-tuning PID controller designed to eradicate tracking error in accordance with user-specified dynamics, and a supervisory controller that functions based on approximate assessments of the system's nonlinearities. Despite their advantages, conventional PID controllers often struggle with tuning parameters in real-time, particularly in the presence of dynamic environmental changes and system uncertainties [10]. Furthermore, a technique described in [11] tackles the

International Journal of
Electrical and Electronics Research (IJEER)
Review Article | Volume 13, Issue 1 | Pages 156-163 | e-ISSN: 2347-470X

trajectory tracking challenge for UAVs. The system comprises an inner block for attitude regulation and an exterior block for position stabilization, employing a total of six PD/PID controllers. A novel nonlinear self-tuning PID controller is proposed to regulate the joint position and link deflection of a flexible-link manipulator (FLM) while accommodating diverse payloads [12]. The FLM parameters are identified in real-time via a recursive least squares technique, while the control parameters are dynamically modified using minimal variance control rules. Additionally, an alternative method outlined in [13] emphasizes the optimization of PID controllers using meta-heuristic methods, including Genetic methods (GAs), the Crow Search Algorithm (CSA), and Particle Swarm Optimization (PSO), to improve quadcopter stability. Further substantial study on quadcopter PID control is available in references [14], [15], [16].

While alternative control systems, such as Model Predictive Control (MPC) [17], Fuzzy Logic Control (FLC) [18], and Sliding Mode Control (SMC) [12], have considerable advantages with respect to nonlinearities, disturbances, and complex dynamics, Though effective for handling constraints and optimizing performance, MPC is computationally intensive and more complex to implement. FLC provides the facility to accommodate uncertainty. However, for specific flying conditions, FLC has to be tuned extensively, while SMC is difficult to realize, and could bring about chattering, PID control is still widely adopted due to its simplicity and ease of implementation, as well as its effectiveness in many practical applications. This paper focused on PID control due to the ease of implementation, previously demonstrated effectiveness in quadcopter control, and because it has been found suitable for systems operating with relatively linear dynamics with small deviations from desired setpoints. Though limited, PID presents a good compromise between performance, computational efficiency, and ease of implementation for the scope of this research, where fast and reliable control is needed for real-time applications.

This study begins with the deriving of the quadcopter's dynamic model, incorporating aerodynamic forces, thrust generation, and the effects of inertia. We then implement the PID control strategy to evaluate its effectiveness in maintaining desired trajectories. The primary contributions of this research include the development of a comprehensive dynamic model that accurately represents the dynamics of the X-configuration quadcopter, considering various external factors; a detailed analysis of the PID control strategy, highlighting its strengths in achieving precise position control; and the establishment of a robust simulation framework using MATLAB/Simulink that allows for extensive testing of the quadcopter's response to disturbances and payload variations. Through these contributions, this research aims to enhance the operational reliability and versatility of X-configuration quadcopters, providing valuable insights for future advancements in UAV technology.

2. MATHEMATICAL MODELLING OF QUADCOPTER

Quadcopters are under-actuated devices that employ four independent inputs to control motion across six degrees of freedom (6-DOF), encompassing three translational and three rotational movements. Their dynamics are markedly nonlinear, mostly owing to aerodynamic effects. Quadcopters provide lift and propulsion via four vertically oriented propellers. They utilize two sets of identical fixed-pitched rotors, with one pair revolving clockwise and the other counterclockwise, arranged diagonally relative to each other [19], [20], [21]. Most quadcopter designs generally exhibit two fundamental configurations: the "+" and "X" formations.

This article examines both configurations, indicating that the "X" arrangement is deemed more stable than the "+" configuration [19], [22], as depicted in *figure 1*. The X-configuration comprises a stiff cross-linked framework including four autonomous rotors fitted with fixed-pitch propellers. In this configuration, two propellers rotate in a clockwise direction while the other two rotate in a counterclockwise direction, as illustrated in *figure 1* [19], [22].

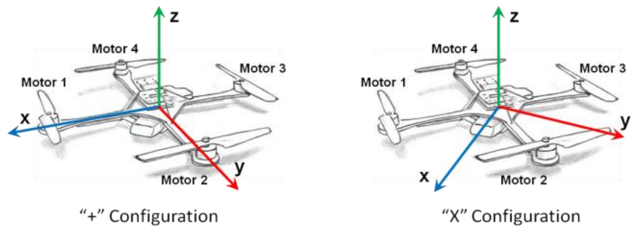

Figure 1. Quadcopter configuration [19]

A big advantage in versatility is the X-configuration drone. Due to symmetrical thrust, it improves stability and control over pitch, roll, and yaw. Its design provides greater agility and is ideal for either racing or filming dynamic scenes. The configuration keeps the camera view clear and unobstructed; hence, it is suitable for photography, videography, surveillance, and others. Aerodynamic efficiency reduces drag, improving both flight performance and battery life, while balanced weight distribution allows it to carry payloads such as cameras or sensors. Besides, this symmetric design minimizes vibration, hence allowing for smoother operations of sensitive equipment, thus making the X-configuration a preferred choice for varied applications. The summarized benefits of X-configuration compared to other configurations can be found in *table 1*.

Table 1. Comparison of drone configurations

Feature	X-Configuration	+-Configuration	H-Configuration	Y-Configuration
Stability	High	Moderate	High	Moderate
Agility	High	Moderate	Moderate	Low

Camera Obstruction	None	Moderate	None	Moderate
Aerodynamics	Efficient	Less efficient	Moderate	Efficient
Weight Distribution	Balanced	Less balanced	Good	Less balanced
Payload Handling	Excellent	Good	Moderate	Limited

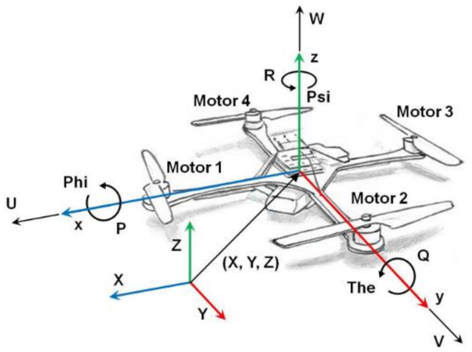

Figure 2. Motion principle for the quadcopter [19]

Modeling a quadcopter is complex due to its elaborate architecture and dynamic systems. This work aims to provide a simple yet pragmatic model of a quadcopter [19], [22], [23], [24].

The cumulative sum of the four forces engaged in altitude regulation is shown as $\mathcal{U}_1$. The mathematical representation of this force is expressed as

$$= c_T(\textstyle\sum_{i=1}^{4} \omega_i^2) \quad (1)$$

where $\omega_i[rad/s]$ is the angular velocity of the propeller i, and c_T $[N.s^2]$ is the impulse coefficient.

To navigate the aircraft laterally, the overall force must be modified proportionately. This rotation enables motion along the Y-axis. $\mathcal{U}_2$ represents the cumulative forces associated with roll rotation and is articulated as follows

$$= C_T l(-\omega_1^2 + \omega_2^2 + \omega_3^2 - \omega_4^2) \quad (2)$$

Where l $[m]$ is the thrusters' distance to the center of mass, for X-configuration$l_x = l \sin(45)$.

To propel the aircraft forward or backward, the cumulative forces produced by the thrusters must be modified correspondingly. This rotation facilitates motion along the X-axis. $\mathcal{U}_3$ represents the total forces involved in the pitch rotation and is expressed as follows.

$$= C_T l(-\omega_1^2 - \omega_2^2 + \omega_3^2 + \omega_4^2) \quad (3)$$

All four thrusters must be employed to effect a change in orientation. $\mathcal{U}_4$ is the aggregate of forces associated with the yaw rotation, expressed as

$$= C_Q(-\omega_1^2 + \omega_2^2 - \omega_3^2 + \omega_4^2) \quad (4)$$

where $c_Q[N.m.s^2]$ is the drag coefficient, Ω represents overall propeller speed which is defined by

$$\Omega = [-\omega_1 + \omega_2 - \omega_3 + \omega_4]^T \quad (5)$$

In *figure 2*, for movement along the *z*-axis, all thrusters must revolve at an identical speed to produce uniform force.

This study outlines the following working hypotheses to elucidate the model dynamics.
(1) The quadrotor's configuration is deemed rigid and symmetrical.
(2) The propellers are supposed to be inflexible.
(3) Thrust and drag forces are directly proportional to the square of the rotor velocity.
(4) The center of mass aligns with the origin of the coordinate system related to the quadrotor construction.

To assess the mathematical model of the quadrotor, we utilize two reference frames: a stationary frame associated with the ground, termed the inertial frame E, and a mobile frame A, with its origin located at the quadrotor's center of mass, as seen in *figure 2*. Altering the rotor speeds modifies the thrust forces Fi=1⋯ 4, leading to the six primary movements as outlined below [20]:

(1) The roll rotation ϕ is succeeded by movement along Ox
(2) The pitch rotation θ is succeeded by movement along Oy
(3) The yaw rotation ψ corresponds to movement along Oz (with represents altitude).

The transformation matrix from the body frame to the aircraft frame can be derived as indicated *in equations (6) and (7)* [20], [25]:

$$\mathcal{R}_\Theta = R(\psi, Z)R(\theta, Y)R(\phi, X) \quad (6)$$

$$\mathcal{R}_\Theta = \begin{bmatrix} c(\psi)c(\theta) & c(\psi)(s\theta)s(\phi) - s(\psi)c(\phi) & c(\psi)s(\theta)c(\phi) + s(\psi)s(\phi) \\ s(\psi)c(\theta) & s(\psi)s(\theta)s(\phi) + c(\psi)c(\phi) & s(\psi)s(\theta)c(\phi) - s(\psi)s(\phi) \\ -s(\theta) & c(\theta)s(\phi) & c(\theta)c(\phi) \end{bmatrix} \quad (7)$$

where $s(\cdot)$ represents the short form of sin(.) and $c(\cdot)$ denote the short form of cos(·) functions.

The Newton-Euler formulation articulates the rotational and translational dynamics in *equation (8)*, with the relevant parameters delineated in *table 2* [20], [25], [26]:

$$\begin{cases} \ddot{x} = (s(\phi)s(\psi) + c(\phi)c(\psi)s(\theta))\frac{\mathcal{U}_1}{m} \\ \ddot{y} = (c(\psi)s(\phi) - c(\phi)s(\psi)s(\theta))\frac{\mathcal{U}_1}{m} \\ \ddot{z} = -g + (c(\phi)c(\theta))\frac{\mathcal{U}_1}{m} \\ \ddot{\phi} = \frac{1}{I_{xx}}\left((I_{yy} - I_{zz})\dot{\theta}\dot{\psi} - J_t\dot{\theta}\Omega + \mathcal{U}_2\right) \\ \ddot{\theta} = \frac{1}{I_{yy}}\left((I_{zz} - I_{xx})\dot{\phi}\dot{\psi} - J_t\dot{\phi}\Omega + \mathcal{U}_3\right) \\ \ddot{\psi} = \frac{1}{I_{zz}}\left((I_{xx} - I_{yy})\dot{\phi}\dot{\theta} + \mathcal{U}_4\right) \end{cases} \quad (8)$$

where $\ddot{x}$, $\ddot{y}$, and $\ddot{z}$ represent the acceleration in the earth fixed coordinate frame (E). ϕ denotes roll, θ is pitch, and ψ represents yaw angles to E. Additionally, m denotes quadcopter mass, g is gravitational acceleration. I_{xx}, I_{yy}, I_{zz} are moments of inertia to A, J_t is the propulsion rotor and propeller moment of inertia. while $\ddot{\phi}$, $\ddot{\theta}$, $\ddot{\psi}$ are angular accelerations to A, and Ω is overall propeller speed is defined as follows:

$$\Omega = \omega_2 + \omega_4 - \omega_1 - \omega_3. \tag{9}$$

Additionally, $\mathcal{U}_1, \mathcal{U}_2, \mathcal{U}_3, and\ \mathcal{U}_4$ are control variables for X-configuration and can be defined as follows:

$$\begin{bmatrix} \mathcal{U}_1 \\ \mathcal{U}_2 \\ \mathcal{U}_3 \\ \mathcal{U}_4 \end{bmatrix} = \begin{bmatrix} c_T & c_T & c_T & c_T \\ -l_x c_T & l_x c_T & l_x c_T & -l_x c_T \\ -l_x c_T & -l_x c_T & l_x c_T & l_x c_T \\ -c_Q & c_Q & -c_Q & c_Q \end{bmatrix} \begin{bmatrix} \omega_1^2 \\ \omega_2^2 \\ \omega_3^2 \\ \omega_4^2 \end{bmatrix} \tag{10}$$

Table 2. Quadcopter parameters

Symbols	Descriptions	Values
c_T	Thrust factor	1.486×10^{-7} N.S^2
c_Q	Drag coefficient	2.925×10^{-9} N.m.S^2
I_{xx}	Inertia moment along the *x* axis	0.0095Kg.m^2
I_{yy}	Inertia moment along the *y* axis	0.0095Kg.m^2
I_{zz}	Inertia moment along the *z* axis	0.0186Kg.m^2
lx	Center distance between the gravity of quadcopter and propeller	0.2223m
m	Total quadrotor's mass	1.023kg
J_t	Rotor Inertia	3.788×10^{-6}Kg.m^2
g	Gravity	9.81m/S^2

3. CONTROLLER ARCHITECTURE

The controller assesses the disparity between the quadcopter's present state and the planned state, producing an error value that it rectifies prior to transmitting outputs. The quadcopter's sensor data are employed to compute this error signal, so completing the feedback loop from output to input. The classical PID controller is extensively utilized because of its obvious tuning procedure, ease of application in the absence of a known system model, and uncomplicated implementation in code with minimum computational demands. This controller generally employs resources commonly found on most onboard systems, as demonstrated in *figure 3* [22], [24].

This study investigated the quadcopter's movement along triangle and square paths to improve stability with a PID control system. The identical control algorithm can be utilized to stabilize the quadcopter while it navigates these trajectories, regardless of whether it is in fly/hover mode or doing other positioning maneuvers. This article details the controller's computation of the intended positions and velocities for the X, Y, and Z axes, predicated on the target values for the quadcopter's movement in each direction. The computed values are subsequently entered into the "Position" block, enabling the controller to continuously adapt and linearize using closed-loop feedback to mitigate any potential error factors.

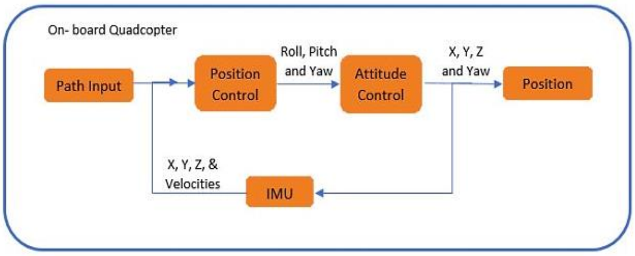

Figure 3. Quadcopter control system architecture [24]

3.1. Attitude Control

The attitude stabilization controller is engineered to preserve the quadcopter's position on the z-axis while stabilizing its roll, yaw, and pitch angles. The stabilization is accomplished with a PID controller that regulates all four degrees of freedom. The altitude stabilization control regulations are based on the methods outlined in [19]. By adeptly managing these parameters, the controller guarantees that the quadcopter remains stable and sensitive to external disturbances, hence improving its overall flight performance. The incorporation of the PID controller facilitates real-time modifications, guaranteeing that the quadcopter can promptly rectify any divergences from its designated path.

$$\phi_{cor} = k_p(\phi_d - \phi) + k_d(\dot{\phi}_d - \dot{\phi}) + k_i \int (\phi_d - \phi)\, dt \tag{11}$$

$$\theta_{cor} = k_p(\theta_d - \theta) + k_d(\dot{\theta}_d - \dot{\theta}) + k_i \int (\theta_d - \theta)\, dt \tag{12}$$

where, ϕ_{cor}, and θ_{cor} are the control output obtained from the controller after correction, ϕ_d and θ_d are the desired roll and pitch for the drone respectively. Also, k_p, k_i, and k_d are tunable PID controller parameters.

The implementation of the controller action for the Z-Axis and also the yaw control. This was achieved by using [19]:

$$\varphi_{cor} = k_p(\varphi_d - \varphi) + k_d(\dot{\varphi}_d - \dot{\varphi}) + k_i \int (\varphi_d - \varphi)\, dt \tag{13}$$

$$\mathcal{Z}_{cor} = k_p(\mathcal{Z}_d - \mathcal{Z}) + k_d(\dot{\mathcal{Z}}_d - \dot{\mathcal{Z}}) + k_i \int (\mathcal{Z}_d - \mathcal{Z})\, dt - g_{offset} \tag{14}$$

where, φ_{cor} and $\mathcal{Z}_{cor}$ are the control output obtained from the controller after correction, φ_d and $\mathcal{Z}_d$ are the desired yaw and position in $\mathcal{Z}$ for the drone respectively. Also, k_p, k_d, and k_i are tunable PID controller parameters.

3.2. Position Control

The position controller, referred to as the outer loop controller, is crucial for supplying reference inputs to the attitude controller, as seen in *figure 3*. It utilizes a basic PD controller to generate orders that direct the quadcopter to its intended location. The controlled state is the inertial-frame velocity, which is directly associated with the quadcopter's attitude modifications. To guarantee precise navigation, positional errors are initially computed in the body frame, enabling the

FOREX Publication
Open Access | Rapid and quality publishing
International Journal of
Electrical and Electronics Research (IJEER)
Review Article | Volume 13, Issue 1 | Pages 156-163 | e-ISSN: 2347-470X

assessment of the quadcopter's distance from its target. The mistakes are subsequently correlated to the target velocity for the body frame, enabling seamless progression towards the objective. The desired velocity is subsequently transformed into requisite attitude modifications, facilitating accurate control of the quadcopter's orientation. Through the integration of these processes, the control system guarantees that the quadcopter can adeptly respond to environmental variations and execute real-time modifications to uphold stability and precision in flight, with the control laws for this intended positioning specified in [19].

$$\theta_d = k_{p1} v_{xerr} - k_{d1} \dot{v}_{xerr} \tag{15}$$

$$\phi_d = k_{d2} \dot{v}_{yerr} - k_{p2} v_{yerr} \tag{16}$$

For *equations (15) and (16)*, the values of v_{xerr} and v_{yerr} are determined in the body frame using the following with the input values of the desired path [19]:

$$v_{xerr} = \mathcal{X}_{err} \cos(\varphi) + \mathcal{Y}_{err} \sin(\varphi) \tag{17}$$

$$v_{yerr} = \mathcal{Y}_{err} \cos(\varphi) - \mathcal{X}_{err} \sin(\varphi) \tag{18}$$

It's worth mentioning that the values of $\mathcal{X}_{err} = \mathcal{X}_{cmd} - \mathcal{X}_{fd}$ and $\mathcal{Y}_{err} = \mathcal{Y}_{cmd} - \mathcal{Y}_{fd}$ are determined to be used in equation (17) and (18). Here $\mathcal{X}_{cmd}$ & $\mathcal{Y}_{cmd}$ are the commanded values for $\mathcal{X}$ & respectively and $\mathcal{X}_{fd}$ & $\mathcal{Y}_{fd}$ are the feedback values obtained from the control loop.

The values of θ_d, ϕ_d, φ_d and z are supplied to the attitude controller. The outputs produced by this controller are subsequently employed to regulate the thrust inputs to the quadcopter's four rotors, facilitating position control and navigation.

3.3. Controller Tuning

Before implementing the feedback control loop, simulations were performed to optimize the PID controller for efficient position tracking of the drone. With the correct configuration of calibrated parameters, the PID control system can precisely track the requested inputs, ensuring minimal error. The PID parameters were tuned via the Ziegler-Nichols approach, as outlined in *table 3*. Utilizing the parameters derived from the initial tuning as a foundation, subsequent simulations aimed at attitude stabilization and position control facilitated the refinement of these parameters. This procedure culminated in the selection of an optimal set of final settings for each integrated PID controller, hence improving the drone's responsiveness and stability in flight [19].

Alternatively, for the PID gain tuning method such as Internal Model Control (IMC) method, Cohen-Coon method, and Genetic Algorithms (GA) can be considered. The IMC method presents a straightforward design procedure because the process model is used in computing the controller parameters. For this reason, performance and robustness can be easily set by a single tuning parameter. The Cohen-Coon method is especially suitable for first-order systems with time delays and has given tuning formulae from step-response data that ensure a balanced and responsive control system. Genetic Algorithms are optimization techniques inspired by natural selection that have proved very effective in determining the optimum PID parameters, especially for complex systems or multi-objective tuning tasks. These methods meet a wide range of system dynamics and ensure precise and reliable control.

Table 3. Tuned parameters

Parameters	$\ddot{\phi}$	$\ddot{\theta}$	$\ddot{\varphi}$	$\dot{\phi}$	$\dot{\theta}$	z
k_p	2	2	4	8	8	130
k_i	0.5	0.5	0.5	0	0	25
k_d	1.2	1.2	3.5	2	2	150

4. SIMULATION RESULTS

The quadcopter's movements were modeled in Simulink, demonstrating the control system's efficacy in maintaining stability along the X and Y axes, as well as ensuring consistent high performance. The results are depicted as the position control answers produced by the control algorithm.

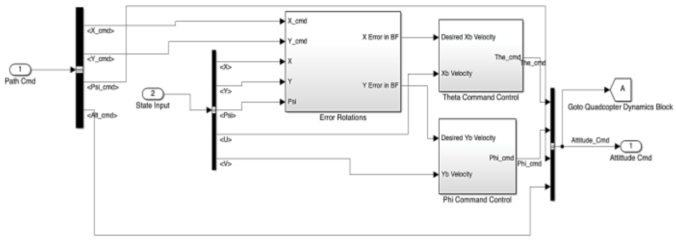

Figure 4. Position control subsystem

4.1. Parallelogram Trajectory

The Path command of position (X_cmd, Y_cmd, Z_cmd) for input to the system as parallelogram trajectory is shown in *table 4* below.

Table 4. Parallelogram position trajectory

Parameters	Unit in meter (m)
X_cmd(m)	[0, 10, 0, -10, 0, 10, 0, 0]
Y_cmd(m)	[0, 0, 10, 0, -10, 0, 0, 0]
Z_cmd(m)	[5, 5, 5, 5, 5, 5, 5, 5]
t(s)	[0, 5, 10, 15, 20, 25, 30, 35]
φ_cmd(rad)	[0]

Modeling of the parallelogram trajectory was conducted by modifying the X_cmd and Y_cmd positions within the horizontal plane, while keeping the Z_cmd height constant at 5 meters, as seen in *figure 5(a).* This elevation also functioned as a reference point. The actual output positions for X and Y were derived via measurements of position or orientation sensors, and these results were juxtaposed with the reference position to evaluate the inaccuracy. *Figure 5(b)* depicts the output position trajectory together with the discrepancies between the desired and actual positions.

FOREX Publication
Open Access | Rapid and quality publishing
International Journal of Electrical and Electronics Research (IJEER)
Review Article | Volume 13, Issue 1 | Pages 156-163 | e-ISSN: 2347-470X

The investigation revealed a positional mistake in the X coordinate, especially evident during the settling time of 0.3 to 2.2 seconds. A minor oscillation of approximately 0.67 meters was noted in the Y position during the settling time from the initiation to 5 seconds. Furthermore, the Z position exhibited an overrun of 0.14m throughout the 15-second settling period. Notwithstanding the discrepancies between the trajectory and the desired position, the control method proved to be effective. A negligible steady-state error was noted for both the X and Y coordinates, accompanied by slight overshooting in the Z position. Consequently, the PID controller was streamlined to a PD controller with integral gain $K_i = 0$ for the X and Y coordinates, but a PID controller was preserved for the Z coordinate.

The comprehensive position and attitude controller was designed to adhere to the parallelogram trajectory, utilizing K_p values of 8 and K_d of 2 for the X (roll) and Y (pitch) position control algorithms, and K_p of 130, K_i of 25, and K_d of 150 for the Z position control algorithms. *Figure 4* illustrates the Simulink subblock diagram for this configuration.

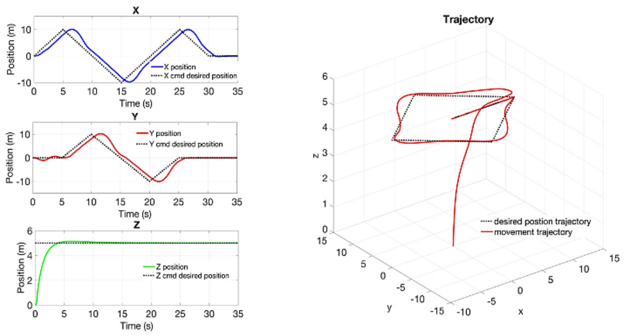

(a) X, Y, and Z position (b) parallelogram movement trajectory

Figure 5. Quadcopter movement with parallelogram trajectory desired

To enhance comprehension of the control coefficients of this quadcopter system, a disturbance parameter denoting a wind speed of 4.15 m/s was incorporated, accompanied by diverse combinations of wind directions applied to the X and Y axes. Figure 6 illustrates the impact of various wind directions on the trajectories of the X and Y positions. The disturbances substantially affected the quadcopter's motion in the X and Y axes, resulting in more pronounced alterations in its trajectory. During the parallelogram motion, under uniform wind influences in the X and Y axes, the PID control system encountered maximum positional deviations of 0.5 meters in the X direction and 0.18 meters in the Y direction. The adjustments caused the quadcopter's flight position to diverge from the intended reference point. As wind velocity escalates, the positional deviation error also amplifies, a principle applicable to all wind direction combinations. Notwithstanding these disruptions, the quadcopter successfully preserved its flight along the parallelogram path. The PID control system is notably adept at addressing disruptions prevalent in real-world contexts, as it is engineered to correct response faults.

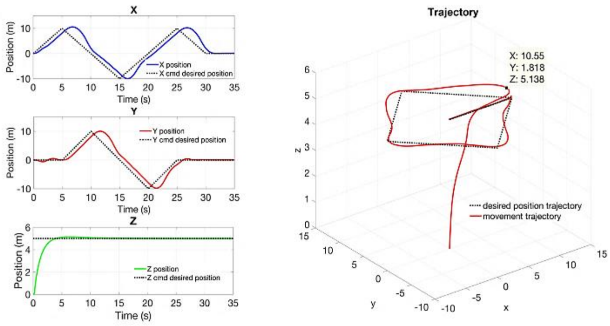

(a) X, Y, and Z position with wind (b) parallelogram movement trajectory with wind

Figure 5. Quadcopter movement with parallelogram trajectory desired by wind load applied

4.2 Triangle Trajectory with Load

The Path command of position (X_cmd, Y_cmd, Z_cmd) for input to the system as a triangle trajectory is shown in *table 5* below

Table 5. Triangle position trajectory

Parameters	Unit in meter (m)
X_cmd(m)	[0, 10, 0, -10, 0, 0, 0, 0]
Y_cmd(m)	[0, 0, 10, 0, 0, 0, 0, 0]
Z_cmd(m)	[5, 5, 5, 5, 5, 5, 5, 5]
t(s)	[0, 5, 10, 15, 20, 25, 30, 35]
φ_cmd(rad)	[0]
Load	0.5kg

The simulation of the quadcopter's movement along a triangular trajectory was performed to study the control coefficients of this design further. A disturbance parameter indicating a wind speed of 4.15 m/s and a load of 0.5 kg was introduced, alongside various combinations of wind directions applied to the X and Y axes, as illustrated in Figure 7. The resultant displacements in the X and Y coordinates attained a maximum of 0.55 meters along the X axis and 0.65 meters along the Y axis. Notwithstanding the wind influences in both directions, the quadcopter successfully sustained its intended trajectory.

The PID control system for the X and Y axes exhibited commendable performance across diverse movement scenarios, as depicted in *figures 6(b)* and *7(b).* The data illustrates the simulation outcomes of the position stabilization control system for the X and Y axes, together with the steady state for the Z axis. Throughout the settling period of 0 to 15 seconds, the position balancing control system successfully maintained the output in alignment with the intended reference. This signifies that the PID system can modify the output location according to various control coefficients. In conclusion, this PID control system is effective within this context, yielding only modest errors in both undisturbed and disturbed settings, hence allowing the quadcopter to successfully follow the required trajectory.

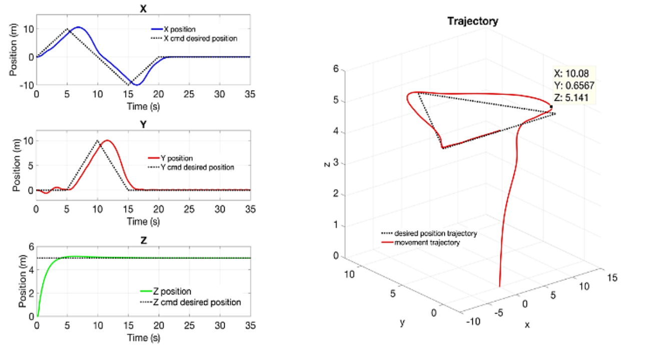

(a) X, Y, and Z position with load **(b)** Triangle movement trajectory with load

Figure 7. Quadcopter movement with triangle trajectory desired by wind and mass load applied

The results indicate a trade-off between marginal error reduction and the processing resources necessary for a finely-tuned controller. This simulation can effectively represent the quadcopter's transition from one position to another with satisfactory stability.

It can be noted that there are minor positional errors and overshooting in the simulation results. These observed positional errors and overshooting in the simulation are likely due to the PID controller's limitations in handling nonlinearities and external disturbances, such as wind or payload changes. PID controllers may struggle with dynamic conditions, leading to overshooting and minor deviations from the desired position.

For future work, FLC-PID could be explored as an alternative. FLC-PID adapts better to nonlinearities and changing conditions by using rules based on real-time feedback, improving performance and reducing overshooting and positional errors. This approach offers greater flexibility and robustness compared to traditional PID controllers.

6. CONCLUSIONS

The mathematical model of the quadcopter motion, kinematic, and dynamic equations were discussed, and the simulation was done with disturbance applied for positioning control. The parameters of the PID controllers were selected to stabilize the deviations from the tuning by using the Ziegler- Nichols method. A closed-loop system was simulated, and the results of the entire process were shown in the MATLAB/Simulink environment with movement trajectories. The results of modeling, simulation, and tuning are quite stable and acceptable with small errors that cannot eliminated, and are easy to implement, which means that they can be used to automate and accelerate various processes in quadcopter research and applications.

For future work, a Fuzzy-PID control strategy will be explored to address the limitations of traditional PID controllers in managing nonlinearities and external disturbances. By combining the adaptability of fuzzy logic with the simplicity of PID control, this hybrid approach aims to improve system performance, reduce positional errors, and enhance robustness in dynamic, real-world environments.

REFERENCES

[1] K. Karam, A. Mansour, M. Khaldi, B. Clement, and M. Ammad-Uddin, “Quadcopters in Smart Agriculture: Applications and Modelling,” *Applied Sciences*, vol. 14, no. 19, p. 9132, Oct. 2024, doi: 10.3390/app14199132.

[2] M. H. Abougabal, M. K. Gamal, M. T. Mohamed Amien, S. O. Mohamed, and A. H. Kassem, “Quadcopter-Rover System for Environmental Survey Applications,” *INCAS BULLETIN*, vol. 16, no. 2, pp. 17–33, Jun. 2024, doi: 10.13111/2066-8201.2024.16.2.2.

[3] J. A. Immanuel Damanik, I. M. Dermawan Sitanggang, F. S. Hutabarat, G. P. Boy Knight, and A. Sagala, “Quadcopter Unmanned Aerial Vehicle (UAV) Design for Search and Rescue (SAR),” in *2022 IEEE International Conference of Computer Science and Information Technology (ICOSNIKOM)*, Laguboti, North Sumatra, Indonesia: IEEE, Oct. 2022, pp. 01–06. doi: 10.1109/ICOSNIKOM56551.2022.10034866.

[4] K. Telli *et al.*, “A Comprehensive Review of Recent Research Trends on Unmanned Aerial Vehicles (UAVs),” *Systems*, vol. 11, no. 8, p. 400, Aug. 2023, doi: 10.3390/systems11080400.

[5] S. Darvishpoor, J. Roshanian, A. Raissi, and M. Hassanalian, “Configurations, flight mechanisms, and applications of unmanned aerial systems: A review,” *Progress in Aerospace Sciences*, vol. 121, p. 100694, Feb. 2020, doi: 10.1016/j.paerosci.2020.100694.

[6] S. Gupte, Paul Infant Teenu Mohandas, and J. M. Conrad, “A survey of quadrotor Unmanned Aerial Vehicles,” in *2012 Proceedings of IEEE Southeastcon*, Orlando, FL, USA: IEEE, Mar. 2012, pp. 1–6. doi: 10.1109/SECon.2012.6196930.

[7] I. Lopez-Sanchez and J. Moreno-Valenzuela, “PID control of quadrotor UAVs: A survey,” *Annual Reviews in Control*, vol. 56, p. 100900, 2023, doi: 10.1016/j.arcontrol.2023.100900.

[8] M. A. Alsaedi, B. M. Albaker, H. A. Dawood, H. Abd Aoun, and Z. K. Tayeh, “Quadcopter Based Object Detection and Localization,” *Iraqi Journal for Computers and Informatics*, vol. 43, no. 1, pp. 40–44, May 2017, doi: 10.25195/2017/4317.

[9] M. Sedighizadeh, A. Rezazadeh, and M. Khatibi, “A self-tuning PID control for a wind energy conversion system based on the Lyapunov approach,” in *2008 43rd International Universities Power Engineering Conference*, Padova: IEEE, Sep. 2008, pp. 1–4. doi: 10.1109/UPEC.2008.4651560.

[10] D. Fister, I. Fister, I. Fister, and R. Šafarič, “Parameter tuning of PID controller with reactive nature-inspired algorithms,” *Robotics and Autonomous Systems*, vol. 84, pp. 64–75, Oct. 2016, doi: 10.1016/j.robot.2016.07.005.

[11] I. Siti, M. Mjahed, H. Ayad, and A. El Kari, “New Trajectory Tracking Approach for a Quadcopter Using Genetic Algorithm and Reference Model Methods,” *Applied Sciences*, vol. 9, no. 9, p. 1780, Apr. 2019, doi: 10.3390/app9091780.

[12] S. K. Pradhan and B. Subudhi, “Position control of a flexible manipulator using a new nonlinear self-tuning PID controller,” *IEEE/CAA J. Autom. Sinica*, vol. 7, no. 1, pp. 136–149, Jan. 2020, doi: 10.1109/JAS.2017.7510871.

[13] A. Sheta, M. Braik, D. R. Maddi, A. Mahdy, S. Aljahdali, and H. Turabieh, “Optimization of PID Controller to Stabilize Quadcopter Movements Using Meta-Heuristic Search Algorithms,” *Applied Sciences*, vol. 11, no. 14, p. 6492, Jul. 2021, doi: 10.3390/app11146492.

[14] U. K. Menon, P. M, and S. S, "Altitude and Attitude Control of X-Configuration Quadrotor Design," in *2023 International Conference on Control, Communication and Computing (ICCC)*, Thiruvananthapuram, India: IEEE, May 2023, pp. 1–6. doi: 10.1109/ICCC57789.2023.10164968.

[15] A. Noordin, M. A. Mohd Basri, Z. Mohamed, and I. Mat Lazim, "Adaptive PID Controller Using Sliding Mode Control Approaches for Quadrotor UAV Attitude and Position Stabilization," *Arab J Sci Eng*, vol. 46, no. 2, pp. 963–981, Feb. 2021, doi: 10.1007/s13369-020-04742-w.

[16] M. A. Lukmana and H. Nurhadi, "Preliminary study on Unmanned Aerial Vehicle (UAV) Quadcopter using PID controller," in *2015 International Conference on Advanced Mechatronics, Intelligent Manufacture, and Industrial Automation (ICAMIMIA)*, Surabaya, Indonesia: IEEE, Oct. 2015, pp. 34–37. doi: 10.1109/ICAMIMIA.2015.7507997.

[17] G. Ganga and M. M. Dharmana, "MPC controller for trajectory tracking control of quadcopter," in *2017 International Conference on Circuit ,Power and Computing Technologies (ICCPCT)*, Kollam, India: IEEE, Apr. 2017, pp. 1–6. doi: 10.1109/ICCPCT.2017.8074380.

[18] A. S. Salem, C. M. Elias, O. M. Shehata, and E. I. Morgan, "Investigation of Various Optimization Algorithms in Tuning Fuzzy Logic-based Trajectory Tracking Control of Quadcopter," in *2020 8th International Conference on Control, Mechatronics and Automation (ICCMA)*, Moscow, Russia: IEEE, Nov. 2020, pp. 82–87. doi: 10.1109/ICCMA51325.2020.9301485.

[19] A. Tiwari, "Position Control of an Unmanned Aerial Vehicle From a Mobile Ground Vehicle," Master of Science in Electrical Engineering, Michigan Technological University, Houghton, Michigan, 2017. doi: 10.37099/mtu.dc.etdr/470.

[20] O. Doukhi, A. R. Fayjie, and D. J. Lee, "Intelligent Controller Design for Quad-Rotor Stabilization in Presence of Parameter Variations," *Journal of Advanced Transportation*, vol. 2017, pp. 1–10, 2017, doi: 10.1155/2017/4683912.

[21] D. Kotarski, Z. Benic, and M. Krznar, "Control Design for Unmanned Aerial Vehicles with Four Rotors," : *Interdiscip. Descr. Complex Syst.*, vol. 14, no. 2, pp. 236–245, 2016, doi: 10.7906/indecs.14.2.12.

[22] K. M. Thu and A. I. Gavrilov, "Designing and Modeling of Quadcopter Control System Using L1 Adaptive Control," *Procedia Computer Science*, vol. 103, pp. 528–535, 2017, doi: 10.1016/j.procs.2017.01.046.

[23] S. Srey and S. Srang, "Adaptive Controller Based on Estimated Parameters for Quadcopter Trajectory Tracking," *IJRCS*, vol. 4, no. 2, pp. 480–501, Apr. 2024, doi: 10.31763/ijrcs.v4i2.1342.

[24] M. M. Eatemadi, "Mathematical Dynamics, Kinematics Modeling and PID Equation Controller of QuadCopter," 2019. [Online]. Available: https://api.semanticscholar.org/CorpusID:201034175

[25] A. A. Najm and I. K. Ibraheem, "Nonlinear PID controller design for a 6-DOF UAV quadrotor system," *Engineering Science and Technology, an International Journal*, vol. 22, no. 4, pp. 1087–1097, Aug. 2019, doi: 10.1016/j.jestch.2019.02.005.

[26] I. Trenev, A. Tkachenko, and A. Kustov, ""Movement stabilization of the parrot mambo quadcopter along a given trajectory based on PID controllers"," *IFAC-PapersOnLine*, vol. 54, no. 13, pp. 227–232, 2021, doi: 10.1016/j.ifacol.2021.10.450.